SURFACE WAVE CONSTRAINTS ON S-WAVE VELOCITY STRUCTURE OF CRUST AND UPPER MANTLE BENEATH SOUTHERN AFRICA

IRIS/UNAVACO Workshop 2003

Angela Marie Larson
Virginia Tech

J. Arthur Snoke
Virginia Tech

David E. James
Carnegie Institution/DTM

Southern African Seismic Experiment (SASE)

Between April 1997 and July 1999, 55 broadband seismographs (REFTEK/STS2) were deployed in southern Africa (see figure 1) as part of a four-year international, multi-institutional, interdisciplinary project (the Kaapvaal Project) to determine the geological processes that led to the formation and stabilization of ancient continental cratons. Approximately half the stations were re-deployed to new sites in April/May 1998 for a total of 81 stations occupied for at least a year. The instruments were sited on bedrock in Zimbabwe, Botswana, and the Republic of South Africa with an average spacing of 100 km. The Archean-age Kaapvaal and Zimbabwe cratons are stable remnants of the Earth's early continental lithosphere. The Limpopo belt is an Archean age collision zone between the two cratons. The Bushveld complex, which is ~2.05 Ga in age and believed to be the world's largest layered intrusion, is also of interest. The effects of this complex appear to have extended well beyond the outcrop area of the intrusion itself. The ~100 km station spacing makes it possible to resolve variations in crustal and upper mantle structure across the major tectonic boundaries of southern Africa from receiver-function and surface-wave inversions.

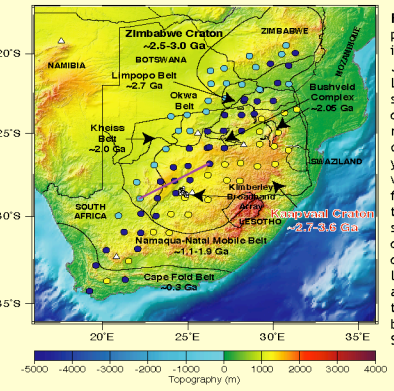

Figure 1: Map showing principle geologic provinces in southern Africa (after James and Fouch, 2002). Locations of the SASE stations are shown as circles: the dark blue circles represent seismographs deployed for the full two years, while stations that were redeployed are shown first as light blue circles and then as yellow circles. The smaller white and black circles within the Kaapvaal craton indicate station locations of the Kimberley array. The purple line marks the interstation path between stations SA16 and SA32 as used in figure 3.

Previous Work

Gore and Nguuri (Ph.D. theses, in preparation) inverted observed surface-wave dispersion velocities for the S-wave structure using events from the first year of the SASE. Gore examined 22 interstation paths from 10 events, and Nguuri used 33 paths from 4 events. Interstation paths had common back azimuths to within 5 degrees of the great circle path, varied in length from 230 to 700 km, and were mostly pure-path within tectonic provinces shown in the map in figure 1. Gore's study area included primarily the Zimbabwe craton and the Limpopo belt. Nguuri also studied the Limpopo belt, as well as the Kaapvaal craton and the Bushveld complex. The major emphasis of both studies was on receiver-function inversion for crustal structure (figure 2), and the surface-wave analysis was used primarily to confirm Moho depths and to supplement tomography results for the uppermost mantle. Figure 3 shows a typical example of the data and inversion for the fundamental mode Rayleigh wave betwen stations SA32 and SA16. Based on the results from linearized least-squares inversion (LLSI), there is a clear incompatibility between models predicted by Love- and Rayleigh-wave inversions performed separately, a consequence presumably of anisotropy.

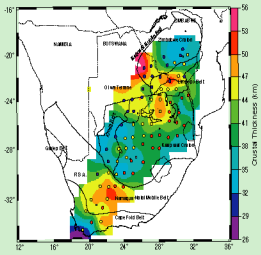

Figure 2: Color-coded contour map of depth to Moho beneath the southern Africa array based on phasing depth images. The crustal-thickness color scale is shown on right. Thin crust tends to be associated with undisturbed areas of craton, particularly in the southern and eastern parts of the Kaapvaal craton and in the Zimbabwe craton north of the Limpopo belt. Greater crustal thickness is associated with the Bushveld region and its westward extension into the Okwa terrane and Magondi belt. Crustal thickness in the central Limpopo Belt was not well constrained by the receiver-function inversion: there were possible Moho conversions at both 30 km and 50 km depths. The surface-wave inversion is consistent with a thicker Moho. The crustal thickness is also greater in the Prot-erozoic Namaqua-Natal mobile belt (from Nguuri *et al.*, 2001).

Figure 3:
Top: The image shows Rayleigh waves recorded on vertical component seismographs at two stations separated by 464 km (see purple line in figure 1) for a magnitude 6.8 event located in central Chile on 15 October 1997. Records have been decimated and instrument corrected for displacement. Seismograms have been low-pass filtered with a corner frequency of 0.05 Hz.
Bottom: This section (from Nguuri's thesis) includes in the left panel the interstation Rayleigh wave phase and group velocities versus period. Data, with phase velocities more heavily weighed than group velocities, have been inverted (using LLSI) to obtain the best-fit S-velocity versus depth model shown as a continuous line in the right panel. The dashed line was the starting model, which was based on the Brazilian craton model shown in figure 5. Nguuri's final model for the Kaapvaal craton does not differ significantly from the one in figure 3. In fact, the mantle portions for all the final models down to 200 km depth do not differ significantly using LLSI-based statistics.

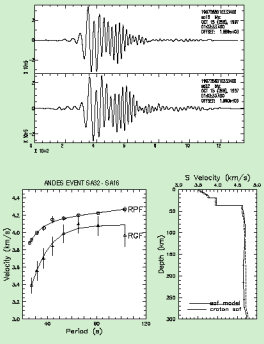

Xenolith Constraints on Seismic Velocities in the Upper Mantle Beneath Southern Africa

James *et al.*, (2003) computed seismic velocities and rock densities from approximately 100 geothermobarometrically calibrated xenoliths from the Archean Kaapvaal craton and adjacent Proterozoic mobile belts. Results for V_p, V_s, and Poisson's ratio are shown in figure 4. Note the comparatively low Poisson's ratio (0.25) in the uppermost mantle as well as the slight decrease in S-wave velocity and increase in P-wave velocity with depth. These velocity constraints, along with densities (not shown), will be used to construct starting models for the upper-mantle velocity structure in the surface-wave inversions.

Figure 4:

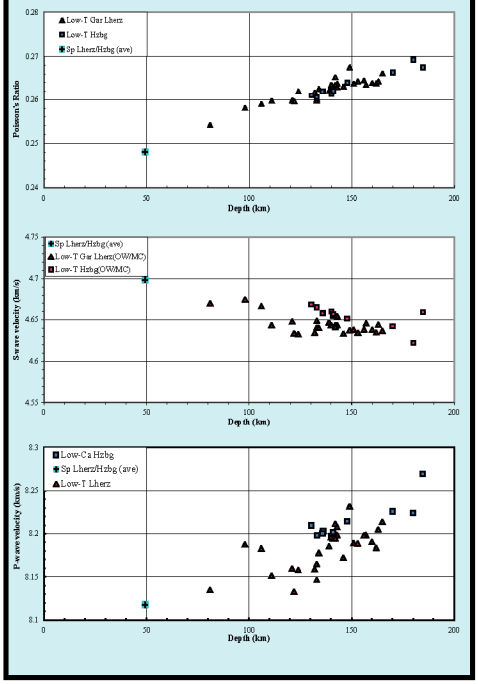

Research Plan

The current research will extend the surface-wave studies by Gore and Nguuri (see Previous Work). Our aim is to improve the constraints on both crustal thickness and upper-mantle velocity structure beneath the different tectonic provinces of southern Africa. We will analyze a substantially larger suite of events (primarily from the second year of SASE) and will include anisotropy in the modeling. The linearized least-squares inversion (LLSI) will be supplemented with an inversion based on the Neighbourhood Algorithm (NA). The NA is a direct-search algorithm for nonlinear inversion that has the benefit of extracting specific data from an ensemble of models as well as determining the best-fit model. Using NA will allow us to test more completely than is possible with LLSI the significance of differences among the regional models and the need to include anisotropy. The NA was used in a smaller-scale study (compared to the current project) of the Brazilian shield (see figure 5). The inversion for velocity structure will make use of xenolith constraints on seismic velocities and densities as shown in figure 4. An additional goal of this research will be to use joint inversion of receiver functions and surface waves to resolve inconclusive results from previous studies of crustal thickness beneath the central Limpopo belt that were based on receiver functions alone.

Application of the Neighbourhood Algorithm (NA) to Brazilian Craton

The NA was applied to invert for the S-wave velocity structure beneath the eastern Paraná Basin (Brazil). The 10,000 evaluations span the space of possible velocity structures and are ranked according to a data misfit criterion. Models were designated as "acceptable" if they had misfits smaller than a value chosen on the basis of the estimated uncertainties of the Rayleigh-wave phase velocities, the best constrained among the dispersion velocities. The statistics of the acceptable model provide a superior measure of significance to that available from LLSI when comparing structures among regions or within a region for different data sets.

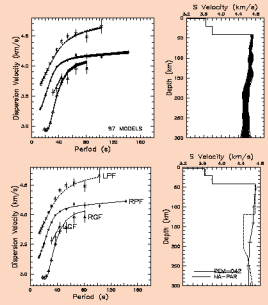

Figure 5: (after figure 5 from Snoke & Sambridge, 2002)
Top: Predicted dispersions and models for the ensemble of all acceptable models from the NA run of 10,000 evaluations. Symbols in the left panel are from the data, averaged over up to four events for each period and mode. Lines are dispersions calculated from the velocity models shown to the right. From top to bottom: Rayleigh group, Rayleigh phase, Love group, Love phase (all fundamental mode).
Bottom: Average model (NA-PAR) and its dispersion calculated from the ensemble shown above. Also shown for reference is the continental PEM model PEM-C42 (Dziewonski *et al.*, 1975).